

Conjugate Heat Transfer Measurements for Air-Cooled Electronics - a New Experimental Method

P. Teertstra, J. P. Urbanski and J. R. Culham
Microelectronics Heat Transfer Laboratory
Department of Mechanical Engineering
University of Waterloo
Waterloo, Ontario, Canada

and

W. Jeakins
Alcatel
Kanata, Ontario, Canada

Abstract

A new method for performing conjugate heat transfer measurements from simulated electronic packages is presented. Using a thermal test component consisting of a foil heater and two calibrated heat flux meters, this new technique provides a means for direct measurement of the heat flow rates in the two predominant paths: convection at the package cap and conduction into the board. A prototype thermal test component was constructed, mounted on four different substrate configurations, and tested in a wind tunnel to demonstrate the effects of varying board conductivity. An energy balance between the heat input and total output measured by the apparatus shows excellent agreement, between 2 and 5% RMS difference, over the full range of velocity and power settings. The proposed method will be used in future studies for heat transfer measurements for arrays of multiple components on thermally conductive substrates.

Nomenclature

A	=	surface area, m^2
A_c	=	cross sectional area, m^2
h	=	convective heat transfer coefficient, W/m^2K
I	=	current, A
k	=	thermal conductivity, W/mK
Q	=	heat flow rate, W
R	=	thermal resistance, K/W
T	=	temperature, $^{\circ}C$
t	=	thickness, m
U	=	approach velocity, m/s
V	=	voltage, V

Greek Symbols

ΔT	=	temperature difference, $^{\circ}C$
θ	=	heat flow ratio, $\equiv Q_{cap}/Q_{brd}$

Subscripts

a	=	ambient
brd	=	board side
cap	=	cap side
in	=	input
l	=	lower (cooled side)
s	=	source
u	=	upper (heated side)

Introduction

To satisfy customer demands for improvements in speed and functionality, electronic manufacturers are continually reducing feature size and increasing circuit density and operating frequency of their products. If not controlled through effective thermal management, the resulting large increases in power density and heat fluxes can result in component temperatures that exceed the limits established for reliable operation. Thermal analysis at the board level during preliminary and final design stages, as well as experimental testing of prototypes and mock-ups, are a critical part of the design process.

The literature contains numerous studies on heat transfer at the circuit board level for a variety of package, substrate and system configurations. Many of these publications containing analytical models, measured data or correlations of empirical results are for the general case of a uniformly sized and spaced array of heated rectangular blocks mounted on one wall of a finite channel. Most of the experimental studies, including Sparrow et al. (1983), Moffat et al. (1985), Souza Mendes and Santos (1987), Buller and Kilburn (1990) and Anderson and Moffat (1992), use a low conductivity material for the substrate, such that any subsequent analysis performed using their data can assume adiabatic conditions at the board. Correlations and analytical models for inline and staggered component arrangements on adiabatic substrates are presented by Anderson (1994), Buller and Kilburn (1990) and Morris and Garimella (1996).

Unlike these previous studies, many current applications rely on conduction through the board, using thick copper ground planes and metallic heat spreaders, to aid in the cooling of high power components. The analytical models and empirical correlations that assume an adiabatic boundary condition on the board are not applicable for the conjugate (coupled conduction and convection) heat transfer that occurs with conductive substrate materials. Of the limited experimental data available for conjugate heat transfer from an array of blocks on a thermally conductive substrate, such as Biber and Sammakia (1996), data are presented for overall heat transfer rate from the blocks only. The experimental procedure followed involves taking measurements of the total heat input into the system, i.e. voltage times current, and a single point temperature measurement on each block. One must infer the effects of adding

conduction or convection enhancement devices, such as heat spreaders or package mounted heat sinks, from their impact on the measured values of Q_{in} and T_s . Using this method it is not possible to directly measure the amount of heat conducted to the board or convected from the package.

The objective of this research study is to develop a new technique for measurement of conjugate heat transfer from a simulated electronic package on a thermally conductive substrate. This method will allow direct measurement of the portion of the total heat flow that is transferred to the substrate via conduction versus that which is convected from the package cap. In this paper, the development of the method and apparatus will be presented, the construction and calibration of a prototype will be described, and wind tunnel testing will be performed to demonstrate the capabilities of the method. The aim of future research studies will be to implement an array of these simulated packages on conductive substrates and provide empirical data for establishing design guidelines and validation of board level models and correlations.

Problem Description

The typical experimental method used in previous studies to measure heat transfer from a simulated package on a substrate is shown in Fig. 1a). An embedded resistance element in the conductive block is used as a heat source, where the total heat flow rate Q_{in} is calculated from direct measurements of voltage and current supplied to the heater:

$$Q_{in} = V \cdot I \quad (1)$$

A single temperature transducer, such as a thermocouple, thermistor or RTD element, is attached to the surface of the block and used to measure T_s . Assuming that the block is isothermal, and that the substrate is adiabatic, the average heat transfer coefficient for the block can be determined by:

$$h = \frac{Q}{A(T_s - T_a)} \quad (2)$$

where A is the total exposed surface area of the block. In the case of a thermally conductive substrate, use of Eq. (2) requires that the portion of heat transferred by convection from the block be determined; however, this quantity cannot be determined using this method.

In the proposed test method the thermally conductive block is replaced by a *thermal test component* (TTC) that contains two calibrated heat flux meters mounted on each side of a planar heat source and covered by a conductive cap, as shown in Fig. 1b). The heat generated by the foil heater follows one of two possible paths; either through the board-side flux meter into the board, or through the cap-side flux meter into the cap. A small air gap between the cap and the board is included in the design to prevent thermal contact between these elements.

The heat flow rate to the cap, Q_{cap} , and to the board, Q_{brd} can be calculated based on measurements of temperature drop across the heat flux meters:

$$Q_{cap} = \frac{\Delta T_{cap}}{R_{cap}} \quad Q_{brd} = \frac{\Delta T_{brd}}{R_{brd}} \quad (3)$$

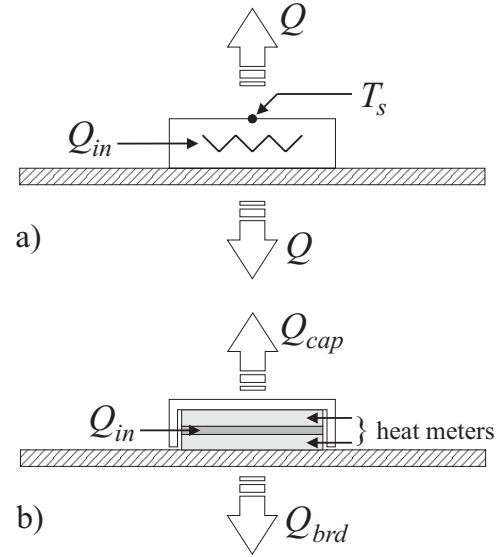


Fig. 1 Schematic of board-level test methods: a) typical apparatus; b) thermal test component method

where ΔT_{cap} and ΔT_{brd} are the differences of the average temperatures on the two sides of the heat flux meters, $T_u - T_l$. Through the use of copper heat spreaders to provide near-isothermal conditions on each of the heat flux meters surfaces, the resistances in Eq. (3) can be determined based on the one-dimensional conduction relationship:

$$R_{cap} = R_{brd} = \frac{t}{kA_c} \quad (4)$$

where t is the thickness of the heat flux meter, A_c is the cross-sectional area and k is the thermal conductivity. A thermal resistance network representation of this model for the heat transfer in the TTC is shown in Fig. 2.

Measurements of Q_{cap} and Q_{brd} from the heat flux meters can be validated using the energy balance:

$$Q_{cap} + Q_{brd} = Q_{in} \quad (5)$$

where Q_{in} is calculated from the voltage and current supplied to the heater. The ratio of the heat transferred to the cap versus that conducted to the board, can be determined by:

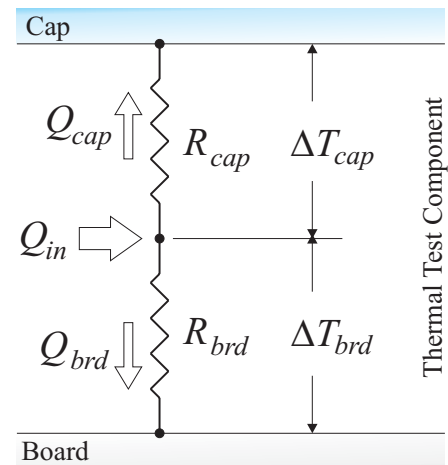


Fig. 2 Thermal resistance network for thermal test component

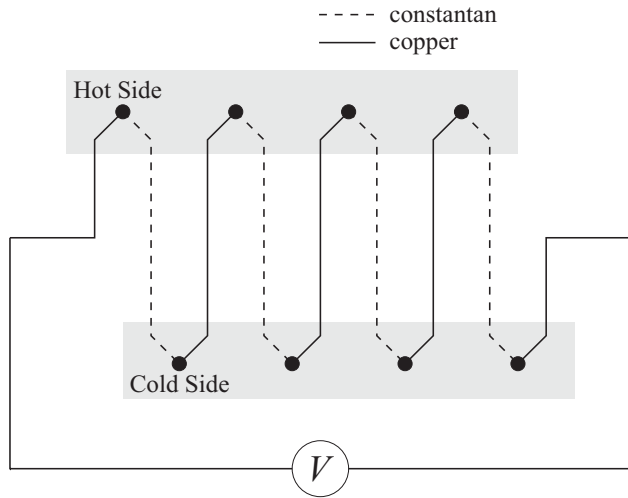


Fig. 3 Schematic of thermopile circuit

$$\theta = \frac{Q_{cap}}{Q_{brd}} \quad (6)$$

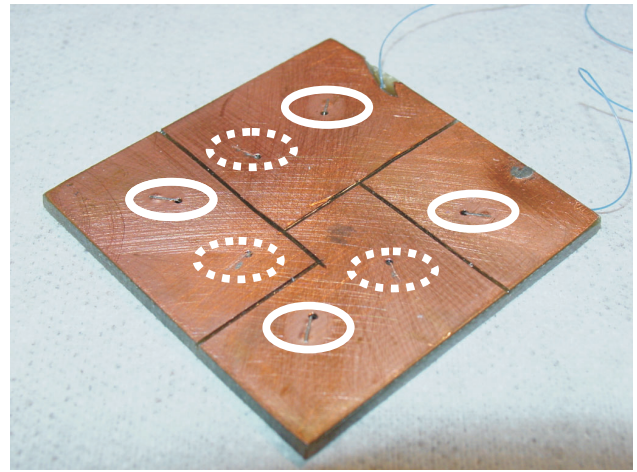
Experimental Apparatus

In order to provide an effective test method and apparatus for future studies involving the use of arrays of thermal test components to simulate board-mounted packages, the following criteria were used in the design of the TTC.

- The dimensions of the thermal test component should reflect those of current packaging technology for high power components. A design and materials should be selected that permit the construction of TTCs with dimensions of $25 \times 25 \text{ mm}$ to $50 \times 50 \text{ mm}$, with thicknesses in the range $2 - 8 \text{ mm}$.
- Materials for the heat flux meter should be chosen that have high tolerances on their dimensions and thermophysical properties to provide accurate measurements. Also, these materials should be relatively inexpensive and the design should be easy to construct to facilitate future testing.
- The technique selected for measuring the temperature drop across the heat flux meter should provide highly accurate results, yet require a minimal amount of wiring and instrumentation to facilitate future tests involving multiple TTCs.

Double sided, 2 ounce copper clad FR4 circuit board was selected as the construction material for the heat flux meters. It is relatively inexpensive, available with a variety of core thicknesses, and has excellent tolerances on both its dimensions and thermophysical properties.

Rather than using a series of thermocouples or similar, single point temperature sensors in the thermal test component, an alternate method for measuring temperature drop across the heat flux meter, the thermopile, was chosen. The thermopile circuit shown in Fig. 3 is a series combination of thermocouple junctions alternating between the hot and cold sides of the system. The resulting potential difference, measured using a



- Copper - constantan junctions
- ⋯ Copper - copper soldered connections

Fig. 4 Prototype heat flux meter

voltmeter, is divided by the number of junction pairs and converted to a temperature difference using available correlations (Omega, 1998). By averaging a number of readings from various locations on the surface, this technique provides very accurate data for the average temperature drop, while maintaining a minimum number of leads and requiring only basic instrumentation to perform the measurements. The thermopile is based on T-type, copper-constantan junctions, where the copper planes on the surfaces of the heat flux meters are used as conductors for the thermopile circuit.

In the case of the prototype heat flux meters constructed for this study, the upper and lower copper layers were divided into four sections, as shown in Fig. 4. Junctions were formed using 30 AWG (0.25 mm) constantan thermocouple wire spot welded to the copper layers at four locations shown in Fig. 4. The remaining three connections shown in Fig. 4 were made using 30 AWG (0.25 mm) copper thermocouple wire soldered to the copper layers. Small diameter 36 AWG (0.13 mm) copper wires were used to connect the heat flux meter to the data acquisition system to minimize conduction losses. All soldered connections and spot welded junctions were lightly sanded to reduce the height of the bead and the completed heat flux meter was dipped in polyurethane to provide electrical insulation.

Heat Flux Meter Calibration

In order to validate the accuracy of the proposed measurement technique, a prototype heat flux meter was constructed and calibrated using an existing thermal interface material test apparatus, as described by Culham et al. (2002) Using the techniques described previously, a $25 \times 25 \text{ mm}$ heat flux meter was constructed using 1.5 mm thick FR4 board material with 2 ounce copper layers. The thermopile was placed between the heat flux meters of the thermal interface material test apparatus using thermal grease at the joints to minimize contact resistance. Once steady state conditions had been achieved, the heat

flow rate through the heat flux meter was measured by the thermal interface material test rig for an average joint temperature of 50 °C:

$$Q = 3.93 \text{ W}$$

The potential difference across the thermopile circuit was measured and converted to a temperature difference in °C using a polynomial expression (Omega, 1998) to give:

$$\Delta T = 18.74 \text{ }^\circ\text{C}$$

Due to the relatively small dimensions of the heat flux meter, heat conduction through the copper wires used in the thermopile circuit cannot be neglected; therefore, the thermal resistance was calculated based on a parallel combination of resistances:

$$R = \frac{1}{\frac{1}{R_{wires}} + \frac{1}{R_{FR4}}}$$

The thermal conductivity of the FR4 material at 50 °C was measured in a separate test using the thermal interface material test apparatus. The heat flow rate predicted by the prototype heat flux meter is:

$$Q = \frac{\Delta T}{R} = 3.99 \text{ W}$$

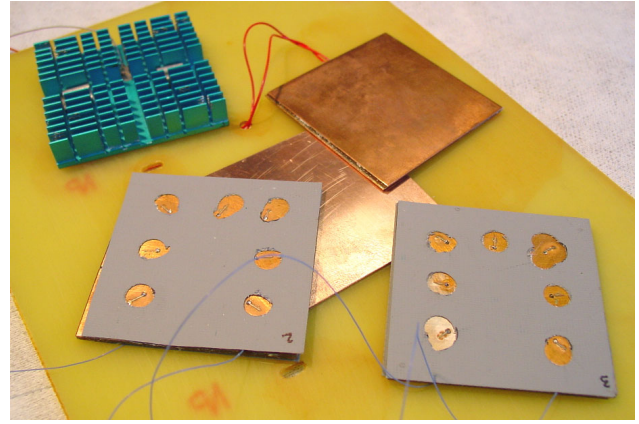
which is less than a 2% difference from the value of Q measured by the interface material test rig.

Wind Tunnel Testing of Prototype Test Component

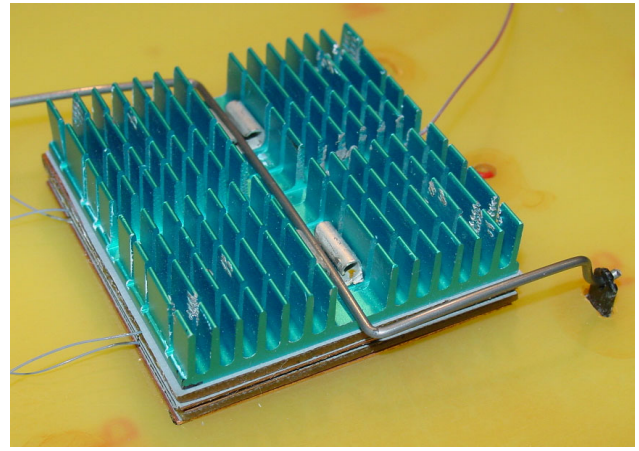
A prototype thermal test component was constructed and tested under natural and forced convection conditions to demonstrate the effectiveness of the proposed method. The objective of these tests was to highlight the significant variations in the heat flow ratio θ that can occur as a function of board conductivity and boundary conditions. The prototype thermal test component used for these measurements is shown in Fig. 5. Due to the preliminary nature of these tests and to avoid machining costs, the cap shown in Fig. 1b) has been replaced by an extruded aluminum heat sink.

Two 50 × 50 mm heat flux meters used in the TTC were constructed of 1.6 mm thick FR4 circuit board material with 2 ounce copper surface layers. The thermal conductivity of the FR4 was determined by testing a 25 × 25 mm sample of board material where the copper layers had been removed by etching. Using the thermal interface material test apparatus (Culham et al., 2002) the conductivity of the FR4 material was measured as $k = 0.373 \text{ W/mK}$ for a joint temperature of 50 °C. The thermopile circuit was created for each heat flux meter as described previously. A 200Ω, 50 × 50 mm kapton foil heater with 0.64 mm thick copper heat spreaders affixed on each side with pressure sensitive adhesive (PSA) was used as the heat source. A similar copper spreader was used at the joint between the board and the heat flux meter, attached to the board using two-sided PSA.

A thin thermal interface material layer was used at all heat flux meter joints to provide additional electrical insulation as well as better thermal contact between the surfaces. Holes were punched in the interface material, as shown in Fig. 5a), to prevent direct contact between the heater or heat sink and the



a)



b)

Fig. 5 Prototype thermal test component: a) components; b) assembly

“bumps” at the spot welded and soldered connections, which could lead to erroneous results.

The heat sink used for the prototype was an extruded aluminum, cross-cut, rectangular fin design from a Pentium desktop computer. The heat sink and all parts of the TTC were clamped firmly to the board using a spring clip, as shown in Fig. 5b). A T-type thermocouple was attached to the heat sink using aluminum filled epoxy, and two additional T-type thermocouples were used to measure ambient air temperature in the test section.

The thermal test component was attached and tested on four different 150 × 200 × 1.6 mm FR4 circuit boards with the following copper layer configurations:

1. bare FR4 board (no copper)
2. one copper layer, TTC mounted on FR4 side
3. one copper layer, TTC mounted on copper side
4. two copper layers

All measurements were performed in a vertical, open circuit wind tunnel with an 46 × 46 × 46 cm test section, as shown in Fig. 6. The boards were positioned at the center of the test section, parallel to the flow direction and gravity vector, and



Fig. 6 Wind tunnel testing of thermal test component

were held in place using monofilament fishing line at each corner. Velocity was measured using a Dantec Flowmaster hotwire anemometer system, and the foil heater was powered by a Xantrex DC power supply. Heater current was measured using a calibrated shunt resistor, and heater voltage was measured using additional leads connected as near to the load as possible. All measurements were performed using a Keithley 2700 data logger, controlled through a GPIB interface by a PC computer. Labview v.5.1 was used for data acquisition and control of the data logger and peripherals.

Measurements were performed for both natural and forced convection, $U = 1, 3$ and 5 m/s , and power levels over the range $3 - 13$ W . The reading of the thermocouple mounted in the heat sink was monitored by the Labview software and steady state conditions were assumed to have been met when the change between 10 subsequent readings at 10 second intervals was less than 0.02% .

Results and Discussion

Table 1 presents heat flow rate data for each of the four test boards, where the energy balance is expressed in terms of a percent difference, calculated based on Q_{in} versus the total heat output:

$$\%diff = \frac{Q_{in} - Q_{cap} - Q_{brd}}{Q_{in}} \times 100\% \quad (7)$$

There is excellent agreement between the energy input and the total heat flow rate measured by the thermal test component for both the natural convection and $U = 1$ m/s cases, with an RMS difference of 1.9% and a maximum difference of 4.1% . More significant differences occur for higher forced convection velocities, $U = 3$ and 5 m/s , where heat losses due to convection from the exposed side surfaces of the thermal test component lead to an underprediction of the total heat flow rate of 4.5% RMS and 7% maximum.

The heat flow ratio, $\theta = Q_{cap}/Q_{brd}$ is presented in Figs. 7 and 8 for each of the four different board configurations, with forced convection data plotted versus approach velocity in Fig. 7 and natural convection data presented in Fig. 8 versus the input power. The values of θ were found to be independent of the input power for each of the forced convection velocities, with a maximum difference between θ values of less than 1% . Therefore, each of the data points plotted in Fig. 7 are average values of θ for the four different input power levels tested, $Q_{in} = 7, 9, 11,$ and 13 W .

The thermal test component has proven very capable of quantifying the effects of enhanced board conduction, clearly demonstrating the significant differences between the heat flow ratios for the bare FR4 board versus board material with copper layers present, both for forced and natural convection. Under forced convection conditions, the heat flow from the heat sink was more than twice that transferred by conduction to the

Table 1 Thermal test component data

U (m/s)	Q_{in} (W)	Bare FR4			1 layer, FR4 side			1 layer, copper side			2 copper layers		
		Q_{cap} (W)	Q_{brd} (W)	% $diff$	Q_{cap} (W)	Q_{brd} (W)	% $diff$	Q_{cap} (W)	Q_{brd} (W)	% $diff$	Q_{cap} (W)	Q_{brd} (W)	% $diff$
NC	2.97	1.65	1.35	-1.1	1.19	1.87	-3.1	1.04	2.06	-4.1	1.06	2.02	-3.7
NC	4.96	2.79	2.22	-0.9	2.03	3.05	-2.4	1.77	3.37	-3.4	1.79	3.31	-2.7
NC	6.95	3.95	3.08	-1.4	2.92	4.20	-2.5	2.51	4.66	-3.3	2.54	4.58	-2.5
1.0	6.96	4.50	2.38	1.3	3.66	3.30	0.1	3.33	3.73	-1.4	3.18	3.83	-0.8
1.0	8.94	5.78	3.07	1.0	4.70	4.24	0.0	4.29	4.79	-1.5	4.09	4.91	-0.7
1.0	10.92	7.06	3.77	0.9	5.78	5.16	-0.2	5.24	5.82	-1.2	4.99	5.98	-0.5
1.0	12.91	8.33	4.50	0.7	6.85	6.11	-0.3	6.19	6.89	-1.3	5.94	7.06	-0.7
3.0	6.97	4.54	2.11	4.6	3.99	2.74	3.5	3.67	3.13	2.4	3.51	3.27	2.7
3.0	8.94	5.78	2.71	5.1	5.12	3.50	3.6	4.70	4.01	2.5	4.50	4.19	2.9
3.0	10.92	7.06	3.32	5.1	6.23	4.29	3.7	5.74	4.91	2.6	5.49	5.12	2.9
3.0	12.91	8.37	3.94	4.6	7.38	5.08	3.5	6.77	5.82	2.5	6.48	6.07	2.8
5.0	6.95	4.37	2.11	6.8	4.02	2.58	5.0	3.75	2.93	4.0	3.60	3.06	4.2
5.0	8.94	5.61	2.71	6.9	5.16	3.31	5.2	4.79	3.76	4.4	4.62	3.93	4.5
5.0	10.93	6.89	3.32	6.6	6.27	4.04	5.6	5.86	4.58	4.5	5.65	4.79	4.4
5.0	12.92	8.12	3.93	6.6	7.43	4.79	5.5	6.93	5.45	4.1	6.64	5.65	4.8

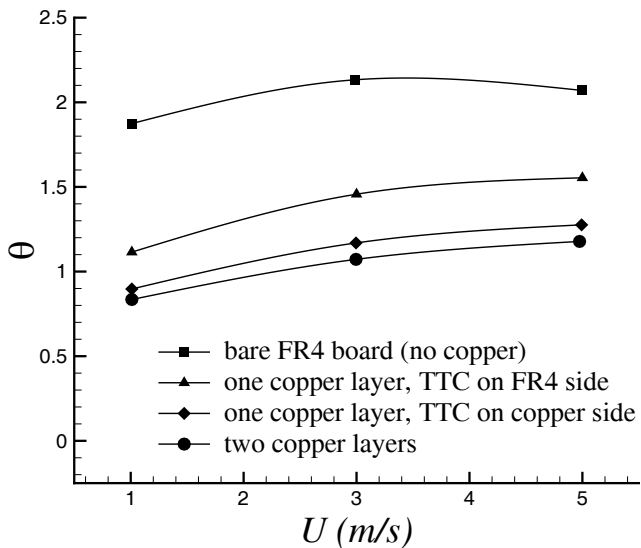


Fig. 7 Heat flow ratio vs. velocity - forced convection

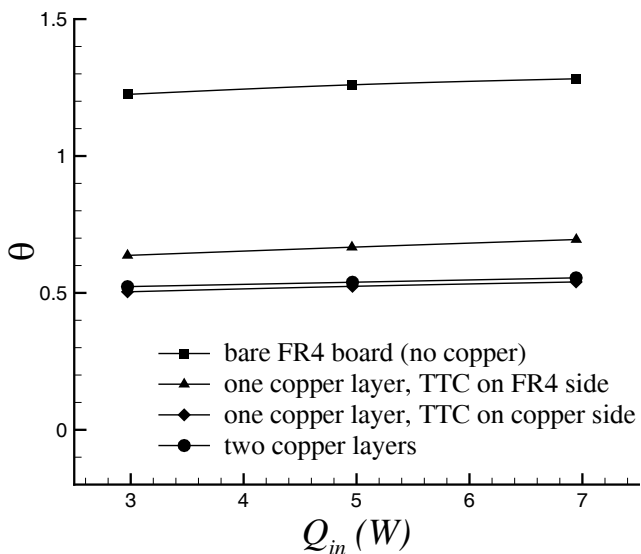


Fig. 8 Heat flow ratio vs. heat flow rate - natural convection

substrate for the bare FR4 board case. As a single copper layer was added, first on the back side of the substrate, then in direct thermal contact with the TTC, the heat flow ratio between the heat sink and board became roughly balanced. For a two layer board under natural convection conditions, a significant amount of the heat transfer from the thermal test component occurs through conduction to the board, almost twice as much as that transferred by the heat sink.

The data shown in Fig. 7 also demonstrate a small effect due to approach velocity. As the velocity increases, the heat sink becomes more effective and the amount of heat transferred to the heat sink increases with respect to that conducted in the board. This behavior is also present to a lesser degree in the natural convection data shown in Fig. 8, where an increase in Q_{in} leads to an increase in the induced velocity in the heat sink and a small, corresponding enhancement in the thermal performance of the heat sink versus conduction in the board.

Summary and Conclusions

A new method has been proposed for the measurement of conjugate heat transfer from a simulated electronic package on a thermally conductive substrate. The proposed thermal test component uses two calibrated heat flux meters to provide direct measurements of the heat flow rate through the two predominant paths, through conduction to the board, and through convection from the cap. The heat flux meter design, which uses a thermopile circuit to measure temperature difference, was calibrated using a thermal interface material test apparatus and has been shown to be accurate to within 2%. A prototype thermal test component was constructed and tested in a wind tunnel using four different circuit board configurations. The energy balance shows excellent agreement between the input power and the measured heat flux values, within 2 - 5% RMS. It is expected that the use of a cap, such that the heater and heat flux meters are not directly exposed to the flow, will reduce this difference.

The thermal test component proved very effective at quantifying the effects of board configuration and boundary conditions on the heat flow ratio, as demonstrated by the results of the wind tunnel tests. The use of the thermopile circuit, readily available materials and simple construction techniques for the thermal test component ensures that this method is suitable for future studies involving arrays of multiple TTCs.

Future research efforts for the thermal test component will involve a number of improvements to the heat flux meters, as follows. In the heat flux meters used in this work, the copper-constantan junctions of the thermopile circuit were all equidistant from the center of the test component. The junctions will be repositioned to better capture the average temperature of the entire surface. Another area for future development involves the techniques used to construct the thermopile circuit, particularly the copper-copper soldered connections. The use of copper plated vias and improved spot welding techniques will be investigated as a means of reducing the size of the "bumps" on the flux meter surface.

Acknowledgments

The authors acknowledge the continued financial support of the Centre for Microelectronics Assembly and Packaging (CMAP) and Materials and Manufacturing Ontario (MMO).

References

- Sparrow, E.M., Vemuri, S.B. and Kadle, D.S., 1983, "Enhanced and Local Heat Transfer, Pressure Drop, and Flow Visualization for Arrays of Block-Line Electronic Components," *International Journal of Heat and Mass Transfer*, Vol. 26, No. 5, pp. 689-699.
- Moffat, R.J., Arvizu, D.E. and Ortega, A., 1985, "Cooling Electronic Equipments: Forced Convection Experiments with an Air-Cooled Array," *Heat Transfer in Electronic Equipment*, HTD-Vol. 48, pp. 17-27.
- Souza Mendes, P.R. and Santos, W.F.N., 1987, "Heat-Transfer and Pressure Drop Experiments in Air-Cooled Electronic-Component Arrays," *Journal of Thermophysics*, Vol. 1, No. 4, pp. 373-378.

Buller, M.L. and Kilburn, R.F., 1990, "Evaluation of Surface Heat Transfer Coefficients for Electronic Module Packages," *Heat Transfer in Electronic Equipment*, HTD-Vol. 20, pp. 25-28.

Anderson, A.M. and Moffat, R.J., 1992, "The Adiabatic Heat Transfer Coefficient and the Superposition Kernel Function: Part 1 Data for Arrays of Flatpacks for Different Flow Condition", *Journal of Electronic Packaging*, Vol. 114, No. 1, pp. 14-21.

Anderson, A.M., 1994, "Decoupling Convective and Conductive Heat Transfer Using the Adiabatic Heat Transfer Coefficient", *Journal of Electronic Packaging*, Vol. 116, No. 4, pp. 310-317.

Morris, G.K. and Garimella, S.V., 1996, "Correlations for Single-Phase Convective Heat Transfer from an Array of Three-Dimensional Obstacles in a Channel," 1996 Proceedings,

5th InterSociety Conference on Thermal Phenomena in Electronic Systems (I-Therm V), Orlando, Florida, May 29-June 1, pp. 292-298.

Biber, C.R. and Sammakia, B.G., 1986, "Transport from Discrete Heated Components in a Turbulent Channel Flow," Presented at the ASME Winter Annual Meeting, Anaheim, California, December 7-12.

Omega, 1998, The Temperature Handbook, Omega Engineering Inc., Stamford, CT, 06907, pg. Z-18.

Culham, J.R., Teertstra, P., Savija, I. and Yovanovich, M.M., 2002, "Design, Assembly and Commissioning of a Test Apparatus for Characterizing Thermal Interface Materials," Eighth Intersociety Conference on Thermal and Thermo-mechanical Phenomena in Electronic Systems, San Diego, CA USA, May 29 - June 1.